

## Measuring CP asymmetry in $B \rightarrow \rho\pi$ Decays without Ambiguities.\*

ARTHUR E. SNYDER AND HELEN R. QUINN

*Stanford Linear Accelerator Center*

*Stanford University, Stanford, California 94309*

### ABSTRACT

We revisit the question of isospin analysis applied to the  $\rho\pi$  decay modes of the  $B$  as a tool to extract the CKM angle between  $V_{ub}^*V_{ud}$  and  $V_{tb}^*V_{td}$ , without ambiguities or uncertainties due to penguin amplitude contributions. We find that a maximum-likelihood fit of the parameters to the full Dalitz plot distribution can successfully extract the parameters—perhaps with as few as 1000 events. This result is from a study of Monte-Carlo-generated events without inclusion of detector efficiency or background effects. The interference between channels is a large effect and provides additional constraints on the parameters compared to channel-by-channel studies. These can usually lift the degeneracy between the multiple solutions that plague such studies. Inclusion of charged  $B$  decays in the analysis would provide a direct check of the Standard Model prediction that the penguin amplitude weak phase for this channel is cancelled by the weak mixing phase.

Submitted to *Phys Rev. D*

---

\* Work supported by the Department of Energy, contract DE-AC03-76SF00515.

## 1. Introduction

Asymmetries in the decays  $B \rightarrow \rho\pi$  can be used to extract a measure of the angle between  $V_{ub}^*V_{ud}$  and  $V_{tb}^*V_{td}$ . This is the angle  $\alpha$  of the “unitarity triangle” derived from the orthogonality of the first and third columns of the three generation Cabibbo-Kobayashi-Maskawa matrix. Together with Lipkin and Nir (LNQS) [1] we pointed out previously the possibility of using an isospin analysis of rates in these channels to extract the angle and eliminate uncertainties due to penguin contributions. Gronau [2] however, stressed that multiple discrete ambiguities would inevitably plague such a treatment. Since measurements of  $\alpha$  from the two pion channel may also suffer from ambiguities due to penguin corrections [3] it would be valuable to have an independent and unambiguous measurement from this channel.

The purpose of this note is to show that such ambiguities can indeed be resolved, provided sufficient data is available to make a full study of the Dalitz plot for the  $\pi^+\pi^-\pi^0$  final states that arise from  $B^0$  and  $\bar{B}^0$  decays. We find that, for most values of the parameters, a 1000 event sample would be sufficient for this analysis, a sample that could reasonably be expected to be collected in a few years of running at a  $B$ -factory.

The interference between  $B^0 \rightarrow \rho^+\pi^0$ ,  $B^0 \rightarrow \rho^-\pi^+$  and  $B^0 \rightarrow \rho^0\pi^0$  can be used to help lift the strong phase/weak phase ambiguity and to determine penguin amplitudes. In addition, with sufficient data, interference makes it possible to resolve the ambiguity [4] between  $\phi_{cp} = \alpha$  and  $\phi_{cp} = 90 - \alpha$  that plagues the study of individual  $B$  channels.

In addition, if charged  $B \rightarrow \rho\pi$  decays can be included in the analysis one can independently fit for the weak phase of the penguin contributions. This would

provide a separate test of the Standard Model prediction that, for this channel, the weak phase of the penguin amplitudes is cancelled by the weak mixing phase. This cancellation will not persist in many models beyond the Standard Model, since additional mixing contributions are a common feature of such models [5]. However, the channel  $\rho^+\pi^0$  has two neutral pions in the final state, and hence this measurement may be quite difficult to make.

In this note we illustrate the power of this method using a maximum likelihood fit to Monte-Carlo-generated samples of  $B \rightarrow \rho\pi$  decays. No detector simulation is included here; detector and background issues have been addressed in Ref. [4]. Our study shows that good fits to the parameters of both the tree and the penguin amplitudes can be obtained with of order 1000  $\rho\pi$  events. For some values of input parameters we found an alternate false solution at  $90 - \alpha$  that gave comparable likelihood to the correct solution for a 1000 event sample, but that was no longer competitive when the event sample was doubled.

The remainder of this note is organized as follows: Section 2 presents the theory, Section 3 describes the event generation and its parameters, Section 4 discusses the fitting procedure, Section 5 presents our results, and Section 6 some conclusions.

## 2. Theory

We use a notation based on that introduced in LNQS for the amplitudes for the various channels. The penguin contributions are identified by the isospin of the final  $\rho\pi$  state to which they contribute. Tree contributions are denoted by  $T^{ij}$  where  $i$  and  $j$  denote the  $\rho$  and  $\pi$  charges respectively. Isospin constraints allow the elimination  $T^{00}$  in terms of the other four.

$$\begin{aligned}
\sqrt{2}A(B^+ \rightarrow \rho^+\pi^0) &= S_1 = T^{+0} + 2P_1 \\
\sqrt{2}A(B^+ \rightarrow \rho^0\pi^+) &= S_2 = T^{0+} - 2P_1 \\
A(B^0 \rightarrow \rho^+\pi^-) &= S_3 = T^{+-} + P_1 + P_0 \\
A(B^0 \rightarrow \rho^-\pi^+) &= S_4 = T^{-+} - P_1 + P_0 \\
2A(B^0 \rightarrow \rho^0\pi^0) &= S_5 = T^{+-} + T^{-+} - T^{+0} - T^{0+} - 2P_0
\end{aligned} \tag{2.1}$$

Similarly for the CP conjugate channels we define the amplitudes  $\bar{S}_i$ ,  $\bar{T}^{ij}$ , and  $\bar{P}_i$  which differ from the original amplitudes only in the sign of the weak phase of each term. In the Standard Model the weak phase of the penguin contributions to this process cancels with the phase of the  $B\bar{B}$  mixing,

$$\arg(q^* P_i \bar{P}_i^*) = 0. \tag{2.2}$$

where  $q$  parameterizes the mixing in the  $B$  mass eigenstates [6],

$$B_H = \frac{B^0 + q\bar{B}^0}{\sqrt{2}}, B_L = \frac{B^0 - q\bar{B}^0}{\sqrt{2}} \tag{2.3}$$

Equation (2.2) is actually an approximation which is correct up to contributions of order  $(m_c^2 - m_u^2)/m_W^2$ . It neglects the kinematic differences in the contributions to the coefficient of the CKM matrix elements for the penguin diagrams with  $c$  and  $u$  quarks in the loop. In our analysis we assume (2.2). Our results for the tree weak phase  $\alpha$  do not depend on this assumption, but the values of the various tree and penguin contributions and their strong phases do. In order to be able determine the weak phase of the penguin contributions in addition to that of the tree contributions one needs to include the charged  $B$  channels in the maximum-likelihood analysis.

In LNQS we considered only the information given by separate time-dependent decay rates in each  $\rho\pi$  channel. A study of the full Dalitz plot and time dependence for  $\pi^+\pi^-\pi^0$  allows the extraction of several further quantities which arise from the interference between the different channels. We denote the Breit Wigner kinematic-distribution functions for the pions produced in the decay of the  $\rho$  by  $f^+$ ,  $f^-$ , and  $f^0$  where the superscript denotes the charge of the decaying  $\rho$ . For  $\rho$  decay to a pion pair of mass  $m$  this function is given by

$$f(m, \theta) = \cos \theta \times 0.5\Gamma_\rho / (m_\rho - m - i0.5\Gamma_\rho) \quad (2.4)$$

where  $m_\rho = 0.77 \text{ GeV}$  and  $\Gamma_\rho = 0.15 \text{ GeV}$ . The dependence on the helicity angle  $\theta$  arises because only  $\rho$ -helicity zero is allowed in the decay  $B \rightarrow \rho\pi$ , since the total spin of the  $\rho\pi$  system must be zero, the spin of the parent  $B$ . This angular dependence ( $|\cos \theta|^2$  in the rates) substantially enhances interference effects, since it increases the number of events in which two of the three possible  $\pi\pi$  pairings both have low invariant mass.

The amplitude for  $B^0 \rightarrow \pi^+\pi^-\pi^0$  can then be written, ignoring non-resonant contributions, as

$$A(B^0) = f^+ S_3 + f^- S_4 + f^0 S_5/2 \quad (2.5)$$

while that for the CP conjugate channel is given by

$$A(\bar{B}^0) = f^- \bar{S}_3 + f^+ \bar{S}_4 + f^0 \bar{S}_5/2. \quad (2.6)$$

A study of the time-dependent Dalitz plots from initial  $B^0$  and  $\bar{B}$  decays in principle allows the measurement of the coefficients of each of the combinations

of time dependent and kinematic functions shown in Table 1. The sign of the  $\sin(\Delta mt)$  terms changes when the initial particle is  $\bar{B}$ .

Now note from (2.1) that

$$S_3 + S_4 + S_5 = T^{+0} + T^{0+} \equiv T$$

and similarly,

$$\bar{S}_3 + \bar{S}_4 + \bar{S}_5 = \bar{T}^{+0} + \bar{T}^{0+} \equiv \bar{T}.$$

The angle between  $T$  and  $\bar{T}$  is precisely  $\alpha$  in the Standard Model, with no ambiguity in its determination.

One can readily check from Table 1 that the Dalitz plot contains sufficient information to determine the magnitudes and phases of the quantities  $S_3, \bar{S}_3, S_4, \bar{S}_4, S_5$  and  $\bar{S}_5$  up to one overall unphysical phase ambiguity. From these one can then extract the quantities  $T, T^{+-}, T^{-+}, P_0$  and  $P_1$  and the weak phase  $\alpha$  between the  $T$  amplitudes and the CP conjugate  $\bar{T}$  amplitudes, given any arbitrary definition of an overall phase convention, and the input assumption, Eq. (2.2), that the weak phase of the penguin contribution is cancelled by the mixing weak phase. In practice the parameters can best be found by using the maximum-likelihood method to fit the full set of parameters to the full Dalitz-plot and time distributions.

The fourth column of Table 1 shows the  $\alpha$  dependence of the tree contributions alone for each term. Note that terms proportional to  $\cos(2\alpha)$  appear from the interference terms. These terms are crucial to the resolution of the ambiguity between  $\alpha$  and  $90-\alpha$  when the penguin contributions are small. Note however these terms vanish when  $T^{+-} = T^{-+}$ , that is when the two different channels happen to have equal amplitudes. For larger penguin contributions the tree-penguin cross

terms are also useful in distinguishing the two angle choices, but again in special cases the ambiguity can remain unresolved.

Since only the combination  $S_1 + S_2 = T^{+0} + T^{0+} = T$  enters for  $B^0$  decays we cannot fit separately for these two amplitudes in this treatment. In an analysis that included charged  $B$  decays two additional parameters would appear (namely, magnitude and phase for the difference of these two amplitudes) and four additional total rates would be measured. Thus if the  $B^+$  decays to  $\rho^+\pi^0$  and to  $\rho^0\pi^+$  and the conjugate  $B^-$  decays can be measured further constraints on the fit will arise from the inclusion of these channels in the maximum-likelihood calculation. Only when these channels are added can the fit determine the weak phase of the penguin contributions in addition to that of the tree contributions. Without the charged channels any value of the penguin weak phase can be accommodated by the fits, by changing the values of the tree and penguin contributions and their strong phases; fortunately, the value of  $\alpha$  extracted is unaltered by such changes.

The check of the expected penguin weak phase cancellation by the mixing phase provides another important test for physics beyond the Standard Model and therefore it is important to attempt this determination. In many extensions of the Standard Model there are additional contributions to the mixing and hence the relationship (2.2) would not hold in such theories [5]. However the  $\rho^+\pi^0$  channel decays to a final state  $\pi^+\pi^0\pi^0$ . This rate may be difficult to measure because of efficiency and background problems in detecting the two neutral pions.

### 3. Monte Carlo Generation of Events

Events are generated with a flat distribution for the  $B \rightarrow \pi^+\pi^-\pi^0$  Dalitz plot, and an exponential time distribution ( $t = -\log_e(R)/\Gamma$ ) and random tag (tag =  $\pm 1$ ). Events are accepted or rejected based on whether a random number is less than or greater than  $|M|^2/|M_{\max}|^2$ , where the amplitude  $M$  is a function of the position on the Dalitz plot, the time  $t$  and whether a  $B^0$  or  $\bar{B}^0$  (tag =  $\pm 1$ ) tag was selected.  $|M_{\max}|$  is chosen so that it is larger than the largest value of  $|M|$  that occurs.  $M$  is constructed as follows: For tag = +1 the time-dependent amplitude is given by

$$M = M_+ = e^{-\Gamma t/2}(\cos(\Delta M t/2)A(B^0) + iq \sin(\Delta M t/2)A(\bar{B}^0)) \quad (3.1)$$

where  $\Gamma$  is the  $B$  decay width and  $\Delta M$  is the mass difference between the heavy and light neutral  $B$  mass eigenstates. The dependence on this quantity arises from the  $B$ - $\bar{B}$  mixing. Similarly for tag = -1 the amplitude is

$$M = M_- = e^{-\Gamma t/2}(q \cos(\Delta M t/2)A(\bar{B}^0) + i \sin(\Delta M t/2)A(B^0)) \quad (3.2)$$

i.e.  $A(B^0)$  and  $A(\bar{B}^0)$  exchange roles.  $A(B^0)$  is given by Eq. (2.5), and  $A(\bar{B}^0)$  by (2.6).

Figure 1 shows an example of the Dalitz plot of a 6500 event sample obtained with this generator. These events were generated with all strong phases set to 0 and with  $\alpha = 20^\circ$ . The penguin amplitudes ( $P_0, P_1$ ) were also set to 0. Tree normalization were taken to be

$$|T| = 0.9 \quad (3.3)$$



and

$$|T^{+-}| = 2|T^{-+}| = 1.0 \quad (3.4)$$

which corresponds to a ‘color-suppression’ factor  $\approx 0.3$  for the  $B^0 \rightarrow \rho^0\pi^0$  amplitude [7]. The clustering in the interference regions where the  $\rho$  bands overlap (the three corners) can clearly be seen. This is caused by the  $|\cos\theta|^2$  dependence discussed above.

In a real experiment the three pion Dalitz plot would receive contributions from non-resonant background and from higher ( $\rho'$ , etc.) resonances. The latter can be removed by a cut which eliminates the kinematically allowed region for such events. Alternately, parametrizations of these additional channels could be included in the fitting procedure and possibly help improve the accuracy of the determination of the weak phase  $\alpha$ . The heavier resonances populate a region corresponding to a smaller triangle inside that populated by  $\rho\pi$  events. As can be seen in Figure 1, cutting out such a region would not remove many  $\rho\pi$  events. Cuts to reduce non-resonant background may also be needed. Our purpose here is not to produce a full study of this problem but rather to demonstrate the power of the Dalitz plot and time distribution analysis to determine the amplitudes. Hence we study only this “ideal” data sample without including backgrounds or the effects of detector resolution and inefficiencies.

## 4. Fitting

We use a maximum likelihood fit to the events generated by the Monte Carlo above to extract an estimate of the parameters and the associated errors. The log-likelihood is given by

$$\log_e L = \sum_i \log_e (|M_i/M_{\text{norm}}|^2) \quad (4.1)$$

where the sum is over generated events,  $M_i$  is the amplitude defined above ( $M_+$ ,  $M_-$ ) in for event  $i$  and  $M_{\text{norm}}$  is a normalization factor. The normalization term is given by

$$|M_{\text{norm}}|^2 = (|N|^2 + |\bar{N}|^2)/2 \quad (4.2)$$

with

$$\begin{aligned} |N|^2 = & (|S_3|^2 + |S_4|^2 + |S_5|^2/4) \langle |f|^2 \rangle \\ & + \text{Re}(2S_3 S_4^* \langle f^+ f^{-*} \rangle + S_3 S_5^* \langle f^+ f^{0*} \rangle + S_4 S_5^* \langle f^- f^{0*} \rangle) \end{aligned} \quad (4.3)$$

and similarly for  $|\bar{N}|^2$  in terms of the  $\bar{S}_i$  amplitudes. Here  $\langle |f|^2 \rangle$  is the square of a Breit-Wigner function averaged over the Dalitz plot and  $\langle f^a f^{b*} \rangle$  is the product of the Breit-Wigner functions for two different charges of  $\rho$  averaged over the Dalitz plot. The averages are calculated using a high statistics Monte Carlo integration.

The parameterization above contains 12 parameters for all  $B^0$  decays to three pions. These are determined as follows:

- The overall phase is not meaningful and is arbitrarily fixed.
- We do not fit for the total rate, which would fix the overall normalization. If acceptances are uniform then this parameter is independent of the remaining

parameters; in a real experiment with non-uniform acceptances it would need to be included in the fitting procedure.

- We fix  $|T^{+-}| = 1$  and set the strong phase for this amplitude  $\delta_{+-} = 0$ . This fixes our overall normalization and phase definitions.
- We input the Standard Model assumption, Eq. (2.2), that the weak phase of the penguin contribution is cancelled by the mixing phase.
- The remaining 9 parameters are determined by the maximum-likelihood fit; these are the weak phase of the tree amplitudes ( $\alpha$ ), the normalization and strong phase for sum of the charged  $B$  decay amplitudes ( $|T|$  and  $\delta_T$ ), the normalization and strong phase for the tree amplitude for  $B^0 \rightarrow \rho^- \pi^+$  decays ( $|T^{-+}|$  and  $\delta_{-+}$ ) and the normalization and strong phases for the  $I=0$  and  $I=1$  penguins ( $|P_i|$  and  $\delta_{P_i}$ ).
- We use MINUIT [8] to maximize the log-likelihood (Eq. (4.1)) as a function of these 9 parameters, using a number of different starting values for the parameters, for each “data” set.

## 5. Results

In order to study the efficacy of this method we have generated 1000 event samples for several different sets of input parameters. We also generated different samples with the same input parameters to test the reproducibility of the results. In addition we generated some larger samples to study how the results improve with increased statistics. We studied a variety of input parameters to test that the sensitivity of the method was not peculiar to a particular choice of input variables. For example if  $\alpha$  is near  $90^\circ$  rates are much more sensitive to penguin effects than

if  $\alpha$  is near  $0^\circ$ . We find similar results for most input parameters, except that ambiguous solutions persist to larger samples when the input parameters include no penguin contribution, or are close to some arbitrary special values that do have ambiguous solutions.

We found that the fitting procedure generally converges to stable set of parameters, but that the result depends on the starting values of the parameters. There are apparently multiple local maxima of the likelihood function and the simple fitting procedure that we used will converge to any one of them. As an example of this for just one of the variables, Figure 2 shows a plot of likelihood versus the weak phase angle  $\alpha$  for the same input parameters as given for Figure 1. In any real experiment a systematic search of parameter space over some reasonable range must be undertaken. In particular when one maximum of the likelihood function is found it is advisable to test the values of the parameters that would correspond to the related ambiguous solutions of a single channel treatment, namely  $\alpha' = 90 - \alpha$ , and  $\cos^2(\delta'_T) = \sin^2(\alpha)$ ,  $\sin^2(\alpha') = \cos^2(\delta_T)$ . The likelihood function may have additional local maxima corresponding to these values.

The cases where the fitting procedure did not converge were readily understood. Most often they corresponded to solutions with very small value for one or more penguin amplitudes and the lack of convergence was due to the inability to define a phase for that quantity. In this cases we simply ran another fit in which the strong phase of the penguin contributions were fixed to zero and this readily converged to a solution.

In one case a the fit generated excessively large contributions to both penguin amplitudes, and then could not then find a satisfactory convergence. This would clearly have been avoided if charged  $B$  data were included in the likelihood fit,

since these depend on only one of the penguin amplitudes.

In Table 2 we tabulate our results for a case where the input penguin amplitudes vanish and all strong phases were set to zero. The table shows the two highest likelihood solutions for the same 1000 event sample and similarly for a 2000 event sample. We find that the ambiguity between  $\alpha$  and  $90 - \alpha$  is not always resolved with a 1000 event sample generated with no input penguin contributions, see Table 2. When the event sample was doubled to 2000 events the results clearly favored the correct angle choice.

If we knew from other evidence, or from improved theoretical calculations, that penguin contributions in this channel can reliably be neglected, then alpha could be determined with smaller errors and, except in special degenerate cases, with no ambiguities even using the smaller event sample. For a number of 1000 event data samples generated with vanishing penguin amplitudes, we tested this by fits in which we fixed all penguin amplitudes to zero. All ambiguities in the asymmetry angle and strong phases were resolved except when  $\pi^+\rho^-$  and  $\pi^-\rho^+$  amplitudes happen to be close to identical. (The degeneracy in this case can be explained by noticing that all  $\cos(2\alpha)$  in Table 1 vanish when these amplitudes are equal.) The error on the angle  $\alpha$  given by these fits was of order  $\pm 1.7^\circ$ . The larger errors shown in Table 2 indicate the additional residual uncertainty due to the inclusion of the additional penguin parameters in the fitting procedure.

When the input parameters included non-zero penguin amplitudes then even with only 1000 events there was no ambiguity as to the best fit, see for example Table 3. In this case the input strong phases were chosen using a random number generator, the maximum likelihood fit does a remarkably good job of obtaining all input parameters from the 1000 event sample, though uncertainties in the strong

phase angles are quite large. We ran fits for a number of other cases with similar results. In general if the input weak phase angle is small we find there is less sensitivity to the penguin contributions, and hence the penguin amplitudes are less well determined. In all our fits we used the Standard Model assumption, Eq. (2.2) for the phase of the penguin amplitudes. However, although the values obtained for all other parameters are sensitive to the assumed penguin weak phase, fortunately the results for the weak phase of the tree diagrams are not. This is because this phase is given directly by the angle between  $T$  and  $\bar{T}$ , while the other quantities can always be chosen to compensate any penguin weak phases in fitting the extracted values of the amplitudes  $S_i$  and  $\bar{S}_i$ .

## 6. Conclusions

We find that the method of fitting isospin amplitudes for tree and penguin contributions to the Dalitz plot and time distributions for three-pion final states using a maximum-likelihood method looks promising. With a thousand Monte-Carlo-generated events we found at worst a two-fold ambiguity in the fit parameters and in many cases a unique choice of best fit parameters that reproduced the input parameters well. The error on the unitarity matrix angle  $\alpha$  is typically of order  $6^\circ$  or less. Penguin contributions and strong phases of all amplitudes were also determined by these fits, though the accuracy of the strong phase determination was poor. (Note that, if we were to assume that the penguin contributions are negligible, this analysis would result in a value for  $\alpha$  with considerably smaller errors, typically of order  $1.7^\circ$ , thus if this assumption could be justified the method would be significantly more powerful. )

When the input value of the penguin contribution was set to zero an ambiguity

between the  $\alpha$  and  $90 - \alpha$  solutions tended to remain. In one case the incorrect solution registered three units of likelihood larger than the correct choice; a warning that solutions with close-by likelihood values should not be too quickly discarded. With a doubling of the samples to 2000 events the results improved to eliminate the incorrect solutions, giving significantly higher likelihood to the fit with parameters close to the input values.

Estimates for the rate of  $\rho\pi$  production from  $B$  decays at a  $B$  factory vary somewhat, but a sample of 1000 events collected over a few years of running seems not an unreasonable estimate. Thus this mode could complement the  $\pi\pi$  mode, not only in determining the angle  $\alpha$  but also in yielding information about the sizes of penguin contributions.

In order to include the charged  $B$  decays in the determination of these parameters one will need to be able to reconstruct  $B^+ \rightarrow \pi^+\pi^0\pi^0$  as well as the easier  $B^+ \rightarrow \pi^+\pi^-\pi^+$ . Further one will need a good understanding of the relative efficiencies for the different charge channels in order to be able to make a combined fit. However the inclusion of the charged channels is needed if one wishes to also determine the weak phase of the penguin contributions for these channels, and thus to test the Standard Model prediction that it is cancelled by the mixing phase.

**Table 1.** The time and kinematic dependence of contributions to the distribution of events.

time dependence	kinematic form	amplitude measured	$\alpha$ dependence (all $P_i = 0$ )
1	$f^+ f^{+*}$	$S_3 S_3^* + \bar{S}_4 \bar{S}_4^*$	1
$\cos(\Delta Mt)$	$f^+ f^{+*}$	$S_3 S_3^* - \bar{S}_4 \bar{S}_4^*$	1
$\sin(\Delta Mt)$	$f^+ f^{+*}$	$Im(q \bar{S}_4 S_3^*)$	$\sin(2\alpha)$
1	$f^- f^{-*}$	$S_4 S_4^* + \bar{S}_3 \bar{S}_3^*$	1
$\cos(\Delta Mt)$	$f^- f^{-*}$	$S_4 S_4^* - \bar{S}_3 \bar{S}_3^*$	1
$\sin(\Delta Mt)$	$f^- f^{-*}$	$Im(q \bar{S}_3 S_4^*)$	$\sin(2\alpha)$
1	$f^0 f^{0*}$	$(S_5 S_5^* + \bar{S}_5 \bar{S}_5^*)/4$	1
$\cos(\Delta Mt)$	$f^0 f^{0*}$	$(S_5 S_5^* - \bar{S}_5 \bar{S}_5^*)/4$	1
$\sin(\Delta Mt)$	$f^0 f^{0*}$	$Im(q \bar{S}_5 S_5^*)/4$	$\sin(2\alpha)$
1	$Re(f^+ f^{-*})$	$Re(S_3 S_4^* + \bar{S}_4 \bar{S}_3^*)$	1
$\cos(\Delta Mt)$	$Re(f^+ f^{-*})$	$Re(S_3 S_4^* - \bar{S}_4 \bar{S}_3^*)$	1
$\sin(\Delta Mt)$	$Re(f^+ f^{-*})$	$Im(q \bar{S}_4 S_4^* - q^* S_3 \bar{S}_3^*)$	$\sin(2\alpha)$
1	$Im(f^+ f^{-*})$	$Im(S_3 S_4^* + \bar{S}_4 \bar{S}_3^*)$	1
$\cos(\Delta Mt)$	$Im(f^+ f^{-*})$	$Im(S_3 S_4^* - \bar{S}_4 \bar{S}_3^*)$	1
$\sin(\Delta Mt)$	$Im(f^+ f^{-*})$	$Re(q \bar{S}_4 S_4^* - q^* S_3 \bar{S}_3^*)$	$\cos(2\alpha)$
1	$Re(f^+ f^{0*})$	$Re(S_3 S_5^* + \bar{S}_4 \bar{S}_5^*)/2$	1
$\cos(\Delta Mt)$	$Re(f^+ f^{0*})$	$Re(S_3 S_5^* - \bar{S}_4 \bar{S}_5^*)/2$	1
$\sin(\Delta Mt)$	$Re(f^+ f^{0*})$	$Im(q \bar{S}_4 S_5^* + q^* S_3 \bar{S}_5^*)/2$	$\sin(2\alpha)$
1	$Im(f^+ f^{0*})$	$Im(S_3 S_5^* + \bar{S}_4 \bar{S}_5^*)/2$	1
$\cos(\Delta Mt)$	$Im(f^+ f^{0*})$	$Im(S_3 S_5^* - \bar{S}_4 \bar{S}_5^*)/2$	1
$\sin(\Delta Mt)$	$Im(f^+ f^{0*})$	$Re(q \bar{S}_4 S_5^* - q^* S_3 \bar{S}_5^*)/2$	$\cos(2\alpha)$
1	$Re(f^- f^{0*})$	$Re(S_4 S_5^* + \bar{S}_3 \bar{S}_5^*)/2$	1
$\cos(\Delta Mt)$	$Re(f^- f^{0*})$	$Re(S_4 S_5^* - \bar{S}_3 \bar{S}_5^*)/2$	1
$\sin(\Delta Mt)$	$Re(f^- f^{0*})$	$Im(q \bar{S}_3 S_5^* - q^* S_4 \bar{S}_5^*)$	$\sin(2\alpha)$
1	$Im(f^- f^{0*})$	$Im(S_4 S_5^* + \bar{S}_3 \bar{S}_5^*)/2$	1
$\cos(\Delta Mt)$	$Im(f^- f^{0*})$	$Im(S_4 S_5^* - \bar{S}_3 \bar{S}_5^*)/2$	1
$\sin(\Delta Mt)$	$Im(f^- f^{0*})$	$Re(q \bar{S}_3 S_5^* - q^* S_4 \bar{S}_5^*)/2$	$\cos(2\alpha)$



**Table 2. Example of fit results with vanishing input penguin amplitudes.**

quantity	input	fit 1	fit 2	fit 3	fit 4
sample size		1000 events	1000 events	2000 events	2000 events
$\alpha$	70	$70 \pm 6$	$31 \pm 6$	$68 \pm 4$	$26 \pm 4$
$ T $	0.9	$0.80 \pm 0.03$	$0.9 \pm 0.1$	$0.9 \pm 0.3$	$0.97 \pm 0.15$
$\delta_T$	0.0	$9 \pm 13$	$3 \pm 8$	$8 \pm 9$	$2 \pm 6$
$ T^{-+} $	0.5	$0.46 \pm 0.03$	$0.25 \pm 0.9$	$0.50 \pm 0.03$	$0.34 \pm 0.11$
$\delta_{-+}$	0.0	$4.6 \pm 3.9$	$5 \pm 12$	$0.2 \pm 3$	$0.2 \pm 7$
$ P_0 $	0.0	$.01 \pm 0.6$	$0.20 \pm 0.11$	$0.02 \pm 0.04$	$0.15 \pm 0.09$
$\delta_{P_0}$	0.0	$171 \pm 66$	$4 \pm 10$	$174 \pm 34$	$-2 \pm 11$
$ P_1 $	0.0	$.05 \pm 0.04$	$0.10 \pm 0.08$	$0.01 \pm 0.01$	$0.08 \pm 0.08$
$\delta_{P_1}$	0.0	$169 \pm 17$	$172 \pm 15$	$97 \pm 184$	$159 \pm 40$
log. likelihood		8739.6	8739.1	17596.6	17590.5

**Table 3. Example of fit results with non-vanishing input penguin amplitudes.**

quantity	input	fit 1	fit 2	fit 3	fit 4
sample size		1000 events	1000 events	2000 events	2000 events
sample size		1000 events	1000 events	2000 events	2000
$\alpha$	70	$65 \pm 6$	$27 \pm 6$	$70 \pm 5$	$19 \pm 6$
$ T $	0.9	$0.91 \pm 0.07$	$1.8 \pm 0.5$	$0.87 \pm 0.05$	$0.92 \pm 0.25$
$\delta_T$	197	$211 \pm 18$	$205 \pm 26$	$208 \pm 17$	$201 \pm 21$
$ T^{--+} $	0.5	$0.44 \pm 0.04$	$0.24 \pm 0.16$	$0.50 \pm 0.03$	$0.24 \pm 0.14$
$\delta_{-+}$	46	$46 \pm 6$	$94 \pm 39$	$41 \pm 4$	$37 \pm 19$
$ P_0 $	0.16	$.21 \pm 0.08$	$0.9 \pm 0.4$	$0.18 \pm 0.04$	$0.51 \pm 0.14$
$\delta_{P_0}$	143	$160 \pm 18$	$86 \pm 17$	$140 \pm 23$	$109 \pm 24$
$ P_1 $	0.18	$.22 \pm 0.04$	$0.8 \pm 0.2$	$0.19 \pm 0.03$	$0.53 \pm 0.09$
$\delta_{P_1}$	97	$123 \pm 13$	$130 \pm 8$	$108 \pm 13$	$137 \pm 10$
log. likelihood		8618.1	8596.7	17079.6	17042.1

## REFERENCES

- [1] H. J. Lipkin, Y. Nir, H. R. Quinn and A. E. Snyder Phys. Rev **D44**, 1454 (1991).
- [2] M. Gronau, Physics Letters **B265**, 389 (1991). Note, a comment in this paper that its Eq. (18) disagrees with Eq. (35) of Ref. [1] is spurious, both equations are correct, there is more than one way to side-step a penguin.
- [3] M.Gronau, SLAC-PUB-5911.
- [4] R. Aleksan, I. Dunietz, B. Kayser and F. Diberder, Nucl. Phys **B361**, 141 (1991).
- [5] C.O. Dib, D. London and Y. Nir, Int. J. Mod. Phys. **A6**,1235 (1991).
- [6] We make here the usual approximation that the difference in lifetimes is negligible and that  $q$  is a pure phase  $q = e^{i\phi_M}$ .
- [7] Complete 'color-suppression' would correspond to the combination of tree amplitudes which enters  $S_5$  (Eq. (2.1)) adding up to 0.
- [8] MINUIT is a program for function minimization and error analysis, developed by F. James and M. Roos, Computer Phys. Comm. **10**, 343 (1975).

## FIGURE CAPTIONS

Figure 1: Sample Dalitz Plot of  $B^0 \rightarrow \rho\pi$ .

Figure 2: Maximum Likelihood as a function of (fixed) fit value of  $\alpha$  for input weak phase  $\alpha = 20^\circ$ .

## TABLE CAPTIONS

Table 1. The time and kinematic dependence of contributions to the distribution of events.

Table 2. Example of fit results with vanishing input penguin amplitudes.

Table 3. Example of fit results with non-vanishing input penguin amplitudes.

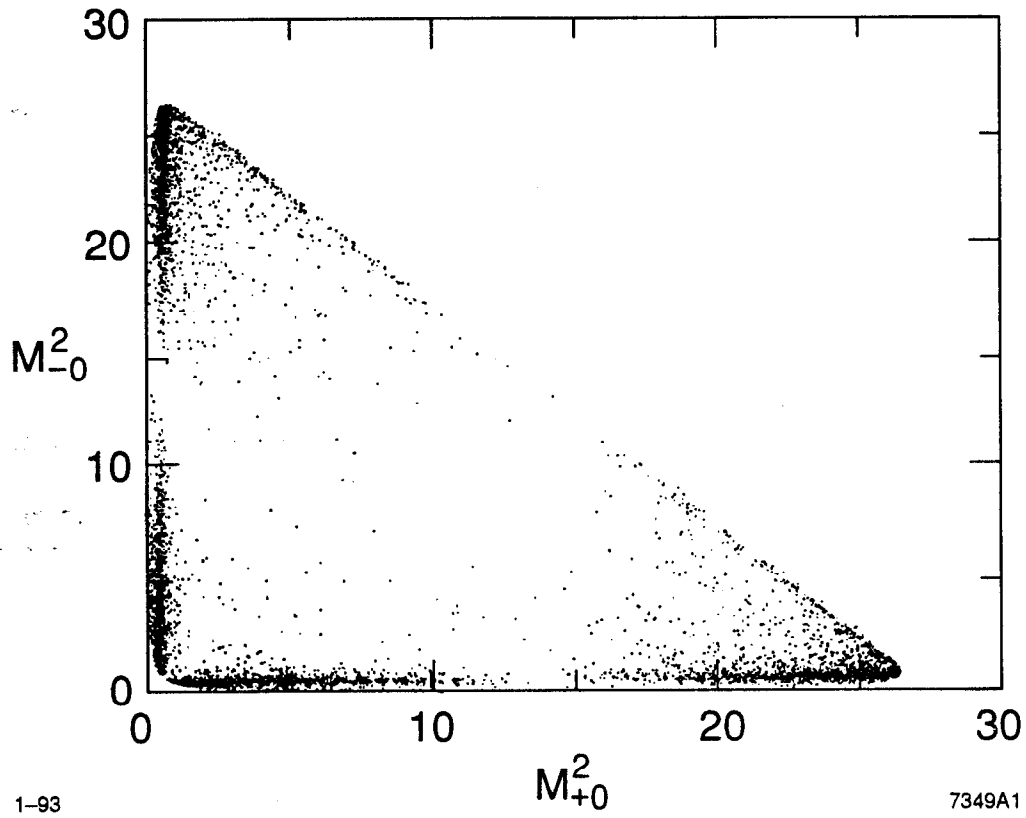


Fig. 1

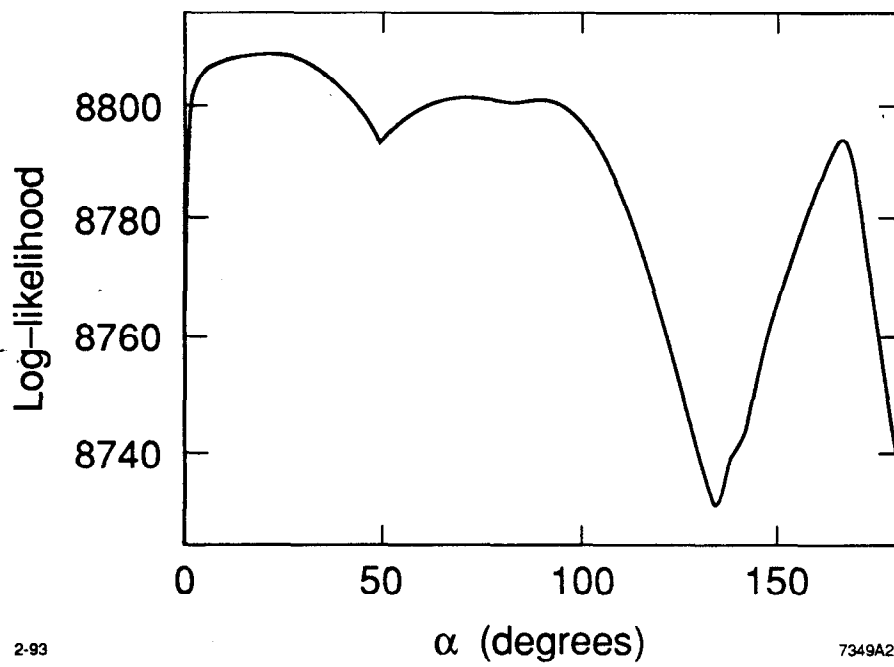


Figure 2